A stochastic model of range profiles of raindrop size distributions: Application to radar attenuation correction

A. Berne and R. Uijlenhoet

Hydrology and Quantitative Water Management Group, Wageningen University, Wageningen, Netherlands

Received 2 November 2004; revised 24 March 2005; accepted 18 April 2005; published 18 May 2005.

[1] To analyze the influence of the spatial variability of the raindrop size distribution (DSD) on rainfall estimation using weather radar, a stochastic model is proposed in order to simulate range profiles of DSDs and consequently profiles of rainfall intensity, radar reflectivity and specific attenuation. A first application concerning the accuracy of attenuation correction algorithms is presented. Using a Monte Carlo technique, it is shown that an attenuation correction algorithm based on a forward implementation is more sensitive to the inadequacy of power-law relations than a backward algorithm, the latter being sensitive to the uncertainty of the path integrated attenuation (PIA). The sensitivity to spatial heterogeneity is limited for both algorithms. The corrected profiles remain uncertain because they are based on deterministic power-law relations which are not fully consistent with the stochastic nature of the DSD. **Citation:** Berne, A., and R. Uijlenhoet (2005), A stochastic model of range profiles of raindrop size distributions: Application to radar attenuation correction, *Geophys. Res. Lett.*, *32*, L10803, doi:10.1029/2004GL021899.

1. Introduction

[2] Climatological, meteorological and hydrological studies require quantitative precipitation estimates. Because of its spatial and temporal resolution as well as the extended coverage, weather radar is very suitable for such purposes. To obtain robust and accurate rainfall estimates using weather radar, the conversion between the radar reflectivity factor Z (in $mm^6\ m^{-3}$) and the rainfall intensity R (in $mm\ h^{-1}$) is a crucial step. Moreover, in the case of C- or X-band wavelengths, the importance of attenuation affecting the radar signal in rain has been recognized for a long time [e.g., *Hitschfeld and Bordan*, 1954]. The launch of airborne and spaceborne radars, operating at even higher frequencies, stimulated the development of novel methods to correct for the attenuation due to rainfall [e.g., *Marzoug and Amayenc*, 1994]. The proposed development of complementary X-band radar networks (e.g., CASA, http://www.casa.umass.edu) is reviving the interest for attenuation correction techniques. Such techniques are based on assumed power-law relations between the integrated radar variables Z, R and k (the one-way specific attenuation, in $dB\ km^{-1}$), which are weighted statistical moments of the raindrop size distribution (DSD). Such power laws have first been empirically established [e.g., *Marshall and Palmer*, 1948]. Later they have been cast in a scaling law framework for analyzing DSDs [*Sempere-Torres et al.*, 1994]. However, all these approaches are based on deterministic relations between stochastic variables [*Haddad and Rosenfeld*, 1997]. To account for the strong variability of rainfall at all scales [e.g., *Jameson and Kostinski*, 2001], in this paper the DSD parameters will be considered as stochastic processes in space.

[3] Adopting a simulation framework allows to produce robust statistics and to perform controlled sensitivity analyses. In this paper, we present a stochastic model to generate range profiles of DSDs and, as an application, a preliminary investigation of the influence of the stochastic variability of the DSD on the accuracy of attenuation correction techniques. We focus on two aspects: (1) the uncertainty due to the use of deterministic power-law relations between the integral variables Z, R and k; (2) the uncertainty due to rainfall heterogeneity within the radar resolution volume (called non-uniform beam filling or NUBF). The present investigation is focused on incoherent single-frequency non-polarimetric radar systems. However, our simulator also provides a potential test bed for multiparameter attenuation correction techniques [e.g., *Testud et al.*, 2000].

2. DSD Profile Simulator

[4] To simulate DSDs in space with realistic features requires the development of a stochastic DSD model. Once a statistical law has been defined for the DSD, profiles can be produced by means of a stochastic process. To generate realistic profiles, the parameters of the stochastic process are deduced from DSD measurements.

2.1. Formulation

[5] To keep the formulation simple and the computation time reasonable, we use an exponential law for the conditional DSD given the parameters N_t (drop concentration) and D_m (mean diameter):

$$N(D|N_t, D_m) = (N_t/D_m)\ \exp(-D/D_m), \tag{1}$$

where D is the diameter and $N(D|N_t,D_m)dD$ represents the number of drops of diameter between D and $D + dD$ per unit volume. Assuming that N_t and D_m follow a bivariate lognormal distribution [*Smith and De Veaux*, 1994] and defining $N' = \ln N_t$ and $D' = \ln D_m$ yields for the joint probability density function:

$$f(N', D') = \mathcal{N}(\mu_{N'}, \mu_{D'}, \sigma_{N'}, \sigma_{D'}, \rho_{N'D'}), \tag{2}$$

where $\mathcal{N}$ denotes the bivariate normal distribution, $\mu_{N'}$ represents the mean of N', $\sigma_{N'}$ its standard deviation (the same notation is used for D'), and $\rho_{N'D'}$ represents the

0094-8276/05/2004GL021899$05.00

Table 1. Mean and Standard Deviation of N_t [m−3] (i.e., per cubic meter), D_m [mm], N' [−] = ln N_t and D' [−] = ln D_m Deduced From HIRE'98 Data at a 2 s Time Step

	N_t	D_m	N'	D'
Mean	4025	0.42	8.1	−0.93
Std	2350	0.14	0.41	0.30

cross-correlation between N' and D'. We are now able to simulate DSDs at one point. One realization is used as the starting point for generating an entire DSD profile. We assume that the stochastic process governing the DSD variability along the profile can be modeled as a discrete stationary vector auto-regressive (VAR) process of order 1:

$$\mathbf{X}[j+1] = \mathbf{C_1}\mathbf{C_0}^{-1}\mathbf{X}[j] + \mathbf{E}[j+1], \tag{3}$$

where

$$\mathbf{X}[j] = \begin{bmatrix} N'(j) - \mu_{N'} \\ D'(j) - \mu_{D'} \end{bmatrix}, \mathbf{E}[j+1] = \begin{bmatrix} \epsilon_{N'}(j+1) \\ \epsilon_{D'}(j+1) \end{bmatrix},$$

$$\mathbf{C_0} = \begin{bmatrix} \sigma^2_{N'} & \sigma_{N'}\sigma_{D'}\rho_{N'D'} \\ \sigma_{N'}\sigma_{D'}\rho_{N'D'} & \sigma^2_{D'} \end{bmatrix},$$

$$\mathbf{C_1} = \begin{bmatrix} \sigma^2_{N'}\rho_{N'}(1) & \sigma_{N'}\sigma_{D'}\rho_{N'D'}(1) \\ \sigma_{N'}\sigma_{D'}\rho_{D'N'}(1) & \sigma^2_{D'}\rho_{D'}(1) \end{bmatrix},$$

j is the distance index, $\rho_{N'}(1)$ represents the auto-correlation at lag 1 (idem for D'), $\rho_{N'D'}(1)$ represents the cross-correlation at lag 1, and $\epsilon_{N'}$ represents a Gaussian white noise process (idem for D'). Therefore $\mathbf{C_0}$ and $\mathbf{C_1}$ are the covariance matrices at lags 0 and 1. The variances of the white noise processes $\epsilon_{N'}$ and $\epsilon_{D'}$ are fixed such that $\mathbf{X}$ is a second order stationary process. It must be noted that the auto-correlation function of a first order VAR is exponential:

$$\rho(j\Delta r) = e^{-\alpha j \Delta r}, \tag{4}$$

where Δr represents the spatial resolution. Once a DSD profile is generated, the corresponding Z, R and k profiles can be deduced, where it is tacitly assumed that the rainfall field can be regarded as a continuum. The model proposed by *Beard* [1976] is used to compute the raindrop terminal fall speed and the Mie theory is used to compute the backscattering and extinction cross sections.

2.2. Parameterization

[6] The statistical model described above has 9 parameters: 5 for the bivariate lognormal distribution ($\mu_{N'}$, $\sigma_{N'}$, $\mu_{D'}$, $\sigma_{D'}$ and $\rho_{N'D'}$) and 4 more for the VAR process ($\rho_{N'}(1)$, $\rho_{D'}(1)$, $\rho_{N'D'}(1)$ and $\rho_{D'N'}(1)$). Let us first focus on the estimation of the parameters for the lognormal distribution. During the HIRE'98 experiment in Marseille, France, DSD measurements have been performed using two optical spectropluviometers, providing DSD time series. As we are interested in the attenuation of the radar signal due to rain, we select a 45 min period during the intense rain event of the 7th of September 1998. Assuming Taylor's hypothesis [e.g., *Fabry*, 1996] with a constant velocity of 12.5 m s^{-1} (consistent with the estimate of [*Berne et al.*, 2004]), we can derive the spatial characteristics of N' and D' we need to parameterize our model. In order to achieve a high resolution of 25 m, the DSD time series has been extracted at a 2 s time step. The parameters N_t and D_m of an exponential law are fitted to the measured diameter spectra, using the third (water content) and sixth (radar reflectivity) order moments of the DSD [*Waldvogel*, 1974]. The obtained values are given in Table 1. They are assumed to be representative despite the significant sampling error present at such short time steps.

[7] Exponential fits of the auto-correlation functions of N' and D' show that $\rho_{N'}(1) = \rho_{D'}(1)$ is a reasonable assumption. The corresponding scale of fluctuation, defined as [*Vanmarcke*, 1983]

$$\theta = \int_{-\infty}^{+\infty} \rho(r)\, dr = \frac{2}{\alpha}, \tag{5}$$

is about 4.2 km, a value consistent with the decorrelation distance of R estimated as about 5 km in a previous analysis of the same event [*Berne et al.*, 2004]. The cross-correlation between N' and D' appears to be negligible, therefore we assume $\rho_{N'D'} = \rho_{N'D'}(1) = \rho_{D'N'} = \rho_{D'N'}(1) = 0$.

[8] As the attenuation effects are more important for X-band wavelengths, we select 3.2 cm as wavelength and the corresponding Mie coefficients have been calculated (at a temperature of 15°C). We simulate DSDs along a range profile of 30 km. As an example of one realization, Figure 1 presents the profiles of the reflectivity factor Z and the corresponding attenuated reflectivity factor Z_a. The mean (over 1000 realizations) of the profile averaged Z, R and k values is 46.5 dBZ, 22.5 mm h^{-1} and 0.46 dB km^{-1}, respectively.

3. Attenuation Correction Algorithms

[9] The DSD model previously described offers an ideal framework to investigate the uncertainty due to the use of deterministic power-law relations between the integral radar random variables in the attenuation correction. We focus on single frequency non-polarimetric radar systems. We shall use two different types of algorithms to analyze the influence of the variability of the DSD. Assuming $Z = ck^d$, we have

$$A(r) = \frac{Z_a(r)}{Z(r)} = \exp\left[-0.2\ln(10)\int_0^r \left(\frac{Z(s)}{c}\right)^{1/d} ds\right], \tag{6}$$

where $A(r)$ is the attenuation factor at the range r ($0 \leq A \leq 1$). *Hitschfeld and Bordan* [1954] (hereinafter

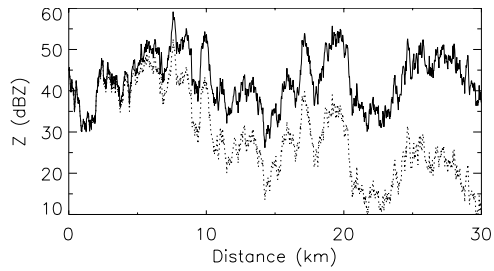

Figure 1. Example of Z (solid line) and Z_a (dotted line) profiles generated by the DSD model.

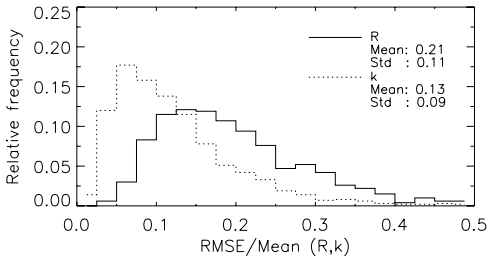

Figure 2. Distribution of the RMSE values, normalized by the mean value over the profiles, calculated between the exact R (k respectively) profiles and the R' (k') profiles obtained by converting the exact Z profiles using the fitted Z-R (Z-k) relations.

referred to as HB) proposed an analytical solution to express A as a function of Z_a:

$$Z(r) = \frac{Z_a(r)}{\left[1 - \frac{0.2\ln(10)}{d}\int_0^r (Z_a(s)/c)^{1/d}\,ds\right]^d}. \quad (7)$$

The HB algorithm is a forward algorithm because the integral is between 0 and r. However, the difference in its denominator can be close to 0 and this makes the algorithm highly unstable.

[10] To avoid instability problems, another family of attenuation correction algorithms has been developed. It is based on the knowledge of the PIA at a given range r_0. The reformulation of equation (7) starting from r_0 and going backward to the radar guarantees the stability of the algorithms. As an example, we use the solution proposed by *Marzoug and Amayenc* [1994] (hereinafter referred to as MA):

$$Z(r) = \frac{Z_a(r)}{\left[A(r_0)^{1/d} + \frac{0.2\ln(10)}{d}\int_r^{r_0} (Z_a(s)/c)^{1/d}\,ds\right]^d}. \quad (8)$$

The main drawback of such a backward algorithm is that it requires a reliable estimation of the PIA at a given range.

[11] To study the accuracy of the algorithms, we use a Monte Carlo technique. One thousand profiles of R, Z and k (hence Z_a) are generated. To study the NUBF effect, the high spatial resolution (25 m) profiles are averaged at a lower spatial resolution (250 m), representing the radar sampling resolution. On each profile a set of power-law relations (Z-R, Z-k) is fitted separately by means of a non-linear regression technique. It must be noted that they constitute the best possible relations. The exact PIA value is calculated as the difference between the non-attenuated and the attenuated Z profiles. Then the two algorithms are applied using the fitted relations on the 1000 high and low resolution profiles.

4. Discussion

[12] The uncertainty due to the use of power-laws for the Z-R (Z-k respectively) relations, independently of the attenuation effect, is quantified via the RMSE values calculated between the exact R (k) profiles and the R' (k') profiles obtained by transforming the exact Z profiles using the fitted Z-R (Z-k) relations. The distributions of the RMSE values, normalized by the mean value of R (k), are plotted in Figure 2. It must be noted that the minimum RMSE value, despite the perfect knowledge of Z and the use of the best possible power-law relations, is always larger than 0: about 2% of the mean k (about 0.01 dB km^{-1}) and about 5% of the mean R (about 1 mm h^{-1}). This value provides a lower limit to the uncertainty of radar rainfall estimation due to Z-R conversion.

[13] The influence of the use of a Z-k power-law relation on the attenuation correction accuracy is analyzed by means of the RMSE values calculated between the exact Z profiles and the Z_c profiles obtained by applying the two attenuation correction algorithms (Figure 3a). The uncertainty increases when the PIA increases for both algorithms. However, the error remains limited for the MA algorithm ($0.01 \leq$ RMSE ≤ 1 in dBZ) when compared to the error for the HB algorithm ($0.01 \leq$ RMSE ≤ 30 in dBZ, plus diverging profiles in about 1 in 4 cases). It must be noted that none of the algorithms is able to achieve a perfect correction, despite the use of the best power-law relations, the exact high resolution Z profiles and the exact PIA in the case of the MA algorithm. This remaining uncertainty is due to the inadequacy of deterministic power-laws to describe the relations between the inherently stochastic DSD weighted moments.

[14] To analyze the impact of NUBF, we first quantify the error due to spatial averaging alone. The averaged Z profiles

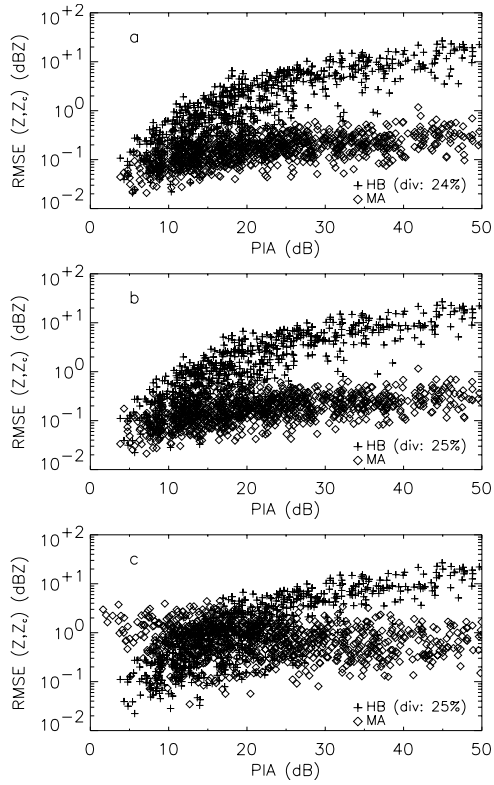

Figure 3. RMSE between the exact Z profiles and the Z_c profiles obtained by applying the two attenuation correction algorithms: (a) 25 m resolution, (b) 250 m resolution, and (c) 250 m resolution with uncertain PIA. 'div' indicates the percentage of diverging HB corrections.

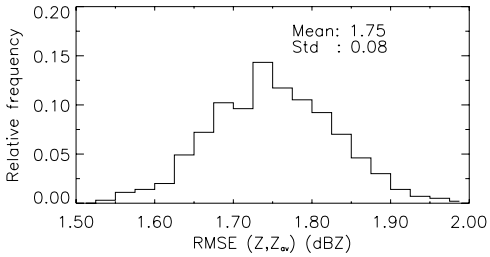

Figure 4. Distribution of the RMSE values calculated at the 25 m resolution between the exact Z profiles and the averaged Z profiles.

are compared to the high resolution Z profiles. Obviously, spatial averaging leads to a significant error, independent of attenuation: the mean RMSE is about 1.75 dBZ (see Figure 4). To quantify the effect of NUBF on the attenuation correction accuracy, the corrected and true Z profiles are compared at the low resolution. The RMSE values calculated at the high and low resolutions are found to be similar (see Figure 3b) for both algorithms. This shows that both attenuation correction schemes do not seem to be sensitive to spatial averaging (from 25 m to 250 m).

[15] To quantify the influence of the possible PIA uncertainty on the performance of the MA algorithm, a Gaussian white noise error (standard deviation of 2.5 dBZ, [*Delrieu et al.*, 1999]) has been added to the exact PIA values. The increase of the RMSE values (see Figure 3c) shows the significant impact of PIA uncertainty on the accuracy of the MA algorithm.

5. Conclusions

[16] A stochastic model has been developed to simulate realistic spatial profiles of DSDs. It is based on an exponential DSD which two parameters follow a bivariate lognormal distribution. The profiles are produced by means of a first order vector auto-regressive process with given correlation characteristics. Intense rain DSD measurements from the HIRE'98 experiment have been used to parameterize the model.

[17] From DSD profiles, it is possible to derive profiles of the variables which are of interest for radar rainfall estimation, i.e. the radar reflectivity factor Z, the rainfall intensity R and the specific one-way attenuation k. Thus a controlled experimental framework has been built to quantify the influence of the stochastic nature of the DSD on the attenuation correction. Focusing on X-band wavelengths, we used a Monte Carlo technique to study the accuracy of two different attenuation correction algorithms. The first (HB algorithm) corresponds to a forward implementation and is known for its instability. The second (MA algorithm) corresponds to a backward implementation and is stable, but requires an additional piece of information which is the PIA at a certain range from the radar. The PIA uncertainty has a strong influence on the accuracy of the MA algorithm.

[18] The non-perfect fit of the power-law relations induces errors, in particular for large PIA, which are small but still significant for the MA algorithm, and which can become huge for the HB algorithm. The results presented correspond to a "best case scenario" and indicate a lower limit for the error remaining after attenuation correction. NUBF, studied by means of spatial averaging, does not seem to have a significant impact on the accuracy of both algorithms. Finally, the proposed model provides a potential test bed to assess the accuracy of recently proposed polarimetric attenuation correction schemes.

[19] We are currently extending our model to be able to deal with three-parameter DSD models (gamma, lognormal). Further research is needed to study different types of precipitation (convective, stratiform, orographic, etc.) and also to extend this work to C-band, which is widely used in operational radar networks. Furthermore, the DSD simulation model offers opportunities to investigate the influence of various sources of error (e.g. radar calibration error, reflectivity measurement inaccuracy) and the question of the sampling error in DSD measurements.

[20] **Acknowledgments.** The authors thank the two anonymous reviewers for their constructive comments. The first author acknowledges financial support from the European Commission through a Marie Curie Postdoctoral Fellowship. The second author is supported by the Netherlands Organization for Scientific Research (NWO). This research is also supported by the EU Projects FLOODsite and VOLTAIRE.

References

Beard, K. (1976), Terminal velocity and shape of cloud and precipitation drops aloft, *J. Atmos. Sci.*, *33*(5), 851–864.

Berne, A., G. Delrieu, J.-D. Creutin, and C. Obled (2004), Temporal and spatial resolution of rainfall measurements required for urban hydrology, *J. Hydrol.*, *299*(3–4), 166–179.

Delrieu, G., S. Serrar, E. Guardo, and J.-D. Creutin (1999), Rain measurement in hilly terrain with X-band weather radar systems: Accuracy of path-integrated attenuation estimates derived from mountain returns, *J. Atmos. Oceanic Technol.*, *16*(4), 405–415.

Fabry, F. (1996), On the determination of scale ranges for precipitation fields, *J. Geophys. Res.*, *101*(D8), 12,819–12,826.

Haddad, Z., and D. Rosenfeld (1997), Optimality of empirical Z-R relations, *Q. J. R. Meteorol. Soc.*, *123*(541), 1283–1293.

Hitschfeld, W., and J. Bordan (1954), Errors inherent in the radar measurement of rainfall at attenuating wavelengths, *J. Meteorol.*, *11*, 58–67.

Jameson, A., and A. Kostinski (2001), What is a raindrop size distribution?, *Bull. Am. Meteorol. Soc.*, *82*(6), 1169–1177.

Marshall, J., and W. Palmer (1948), The distribution of raindrops with size, *J. Meteorol.*, *4*, 186–192.

Marzoug, M., and P. Amayenc (1994), A class of single- and dual-frequency algorithms for rain-rate profiling from a spaceborne radar. part I: Principle and tests from numerical simulations, *J. Atmos. Oceanic Technol.*, *11*(6), 1480–1506.

Sempere-Torres, D., J. Porrà, and J. Creutin (1994), A general formulation for raindrop size distribution, *J. Appl. Meteorol.*, *33*(12), 1494–1502.

Smith, J., and R. De Veaux (1994), A stochastic model relating rainfall intensity to raindrop processes, *Water Resour. Res.*, *30*(3), 651–664.

Testud, J., E. Le Bouar, E. Obligis, and M. Ali-Mehenni (2000), The rain profiling algorithm applied to polarimetric weather radar, *J. Atmos. Oceanic Technol.*, *17*(3), 332–356.

Vanmarcke, E. (1983), *Random Fields: Analysis and Synthesis*, 382 pp., MIT Press, Cambridge, Mass.

Waldvogel, A. (1974), The N_0 jump of raindrop spectra, *J. Atmos. Sci.*, *31*(4), 1067–1078.

A. Berne and R. Uijlenhoet, Wageningen University, Hydrology and Quantitative Water Management Group, Nieuwe Kanaal 11, NL-6709 PA Wageningen, Netherlands. (alexis.berne@wur.nl)